

To write down mathematical expressions for all these things would not add much to the discussion, because the volume of the numerical calculations that were done would make it impossible to present them. These calculations are detailed at greater length in reference 1 for those persons particularly interested. The results of these calculations are

$$\begin{aligned} B/A &= 0.140\text{—flip} \\ &= 0.00816\text{—no flip,} \\ C/A &= 0.215\text{—flip} \\ &= 0.228\text{—no flip,} \\ D/A &= 0.0427\text{—flip} \\ &= 0.0078\text{—no flip.} \end{aligned}$$

These results are plotted and compared with the experimentally measured numbers in Fig. 7.

## CONCLUSIONS

This experiment seems to indicate an interaction intermediate between all flip and no flip. Or, saying this another way, we can “explain” the experimental result within the framework of the theory used here by a proper choice of the ratio between flip and no-flip amplitudes.

## ACKNOWLEDGMENTS

It is a pleasure for us to acknowledge many helpful discussions with Dr. R. E. LeLevier, and in addition the wholehearted cooperation and support of all the people and services at the University of California Radiation Laboratory, Berkeley, that helped to make this experiment possible.

## Study of the Interaction of Positive $K$ Mesons\*

JOSEPH E. LANNUTTI,† SULAMITH GOLDBABER, GERSON GOLDBABER, AND WARREN W. CHUPP,  
*Radiation Laboratory and Department of Physics, University of California, Berkeley, California*

AND

S. GIAMBUZZI, C. MARCHI, G. QUARENI, AND A. WATAGHIN,  
*Istituto Di Fisica “A. Righi,” Della Università Degli Studi Di Bologna, Bologna, Italy*

(Received November 22, 1957)

Continuing our program on the study of positive  $K$  mesons, we have investigated the interactions of  $K$  mesons with hydrogen and complex nuclei in photographic emulsions primarily in the energy interval 100 to 220 Mev. We are reporting on interactions found in 320 meters of  $K^+$  track length followed, of which 227 meters were in the energy interval 100 to 220 Mev. The exposure was made to an enriched  $K$ -meson beam at the Berkeley Bevatron. The ratio of  $K$  mesons to minimum ionizing background particles ranged from 1:1 to 1:3 across our stack. Thirteen new  $K$ -hydrogen scattering events were found and added to those previously published. We find the  $K$ -H cross section to be energy-independent in the energy interval from 20 to 200 Mev. The average cross section over this energy interval is  $14.5 \pm 2.2$  mb. The differential cross section appears to be due predominantly to  $S$ -wave scattering.

The data obtained on inelastic collisions with complex nuclei have been analyzed by using an independent-particle model for the nucleus. Using this model and correcting for (a) nucleon shading, (b) Coulomb repulsion, (c) Pauli exclusion principle, and (d) repulsive potentials, we obtained the average  $K$ -nucleon

cross section as a function of energy. This cross section appears energy-independent in the energy interval 60 to 180 Mev. The values for the elementary cross sections obtained in this analysis for  $T_K=60$  to 180 Mev with  $V=V_N+V_C=35$  Mev were  $\bar{\sigma}$  (the average  $K$ -nucleon cross section)  $=11.8 \pm 1.3$  mb,  $\sigma_{KN}=9.8 \pm 3.0$  mb (with  $\sigma_{Kn}=\sigma_{n^+}+\sigma_{n^0}$  where  $\sigma_{n^+}$  is direct neutron scattering and  $\sigma_{n^0}$  is charge-exchange scattering),  $\sigma_{n^+}=5.8 \pm 3.1$  mb, and  $\sigma_{n^0}=4.0 \pm 0.8$  mb. In this case the ratio  $\sigma_{Kn}:\sigma_{n^+}:\sigma_{n^0} \approx 3.6:1.5:1$ . We observe a backward peaking in the differential cross section and believe that this is due to a small  $P$ -wave contribution.

These results lead us to believe that the  $K$ -nucleon scattering is a short-range force interaction and does not proceed through single  $\pi$ -meson exchange. The latter would require high-angular-momenta contributions and would presumably result in a strongly energy-dependent cross section.

A repulsive potential was necessary to explain the behavior of the fractional energy loss as a function of energy. The magnitude of the potential necessary for a best fit  $V \approx 30$  Mev agrees very well with the results of a partial wave analysis of the elastic-scattering data.

## I. INTRODUCTION

CONTINUING our program<sup>1,2</sup> on the study of positive  $K$  mesons, we have investigated the interaction

\* This work was done under the auspices of the U. S. Atomic Energy Commission.

† Now at Florida State University, Tallahassee, Florida.

<sup>1</sup> Chupp, Goldhaber, Goldhaber, Iloff, Lannutti, Pevsner, and Ritson, *Proceedings of the 1955 Pisa Conference* [Suppl. Nuovo cimento 4, 361 (1956)].

<sup>2</sup> Chupp, Goldhaber, Goldhaber, Helmy, Iloff, Lannutti, Pevsner, and Ritson, *Phys. Rev.* **101**, 1617 (1956).

of  $K$  mesons with hydrogen and complex nuclei in photographic emulsion primarily in the energy interval 100 to 220 Mev. The exposure was made to an enriched  $K$ -meson beam at the Bevatron. The  $K$ -hydrogen scattering events found have been added to those previously published and the improved cross section and angular distribution is discussed. The data obtained on the inelastic collisions with complex nuclei have been analyzed by using an independent-particle model for the nucleus from which the  $K$ -nucleon cross section

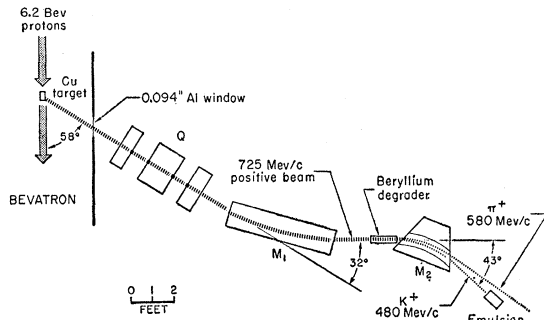


FIG. 1. Schematic drawing of exposure system.

was deduced. It was also possible to obtain an estimate of the  $K$ -neutron elastic and charge-exchange cross section. The observed energy loss of the positive  $K$  mesons is shown to be consistent with a repulsive nuclear potential. A discussion of the ratio of charge-exchange to noncharge-exchange scattering as well as the angular momentum states involved in the scattering process is given in the last section of this paper. In the following paper<sup>3</sup> the elastic scattering of  $K^+$  mesons is analyzed.

## II. EXPERIMENTAL DETAILS

### A. Exposure

In this experiment we used a partially separated positive  $K$ -meson beam. We were able to obtain a ratio of  $K$  mesons to minimum-ionizing background particles ranging from 1:1 to 1:3 across our stack. This is to be compared with a  $K:\pi$  ratio of  $\sim 1:100$  in an unseparated beam.

The separation scheme used consisted of a double-focusing magnet system with an energy degrader between the magnets. This system was designed, in cooperation with D. H. Stork of the University of California at Los Angeles, for  $K$  mesons with energies up to 200 Mev. The physical setup is shown in Fig. 1.

Particles emitted at approximately  $60^\circ$  from a copper target enter a system of three 4-inch quadrupole lenses  $Q$  and are deflected through an angle of  $32^\circ$  by an analyzing magnet  $M_1$ . The particles then pass through an 18.5-inch Be degrader ( $87 \text{ g/cm}^2$ ) and finally are deflected by a magnet  $M_2$  through  $42^\circ$ . The system was tuned so that positive particles of momentum  $725 \pm 23 \text{ Mev}/c$  were incident on the degrader. The degrader reduced the  $K$ -meson momentum to  $480 \pm 30 \text{ Mev}/c$  and the pion momentum to  $580 \text{ Mev}/c$ . With these momenta and magnet  $M_2$  set at maximum field, the central pion trajectory was 6 inches from the central  $K$ -meson trajectory at the stack position. The total distance from the target to the stack was 24.3 ft. The total time of flight was

$1.9 \times 10^{-8}$  sec. The exposure was carried out for  $4.7 \times 10^{13}$  protons on the target. The stack exposed consisted of 129 (4-inch  $\times$  7-inch  $\times$  600  $\mu$ ) Ilford G-5 emulsions.

The yield for this system was approximately ten  $K$  mesons per  $10^{10}$  protons on the target over an area of about  $250 \text{ cm}^2$ . The background of lightly ionizing particles striking the emulsions in the beam direction consisted of pions, muons, and electrons. In the center of the beam there was about one lightly ionizing track per  $K$  meson, and this ratio increased by a factor of about three on the side of the stack nearest the separated pion beam. The proton contamination having the same grain density as the  $K$  mesons was less than 2%. This was easily identified by ionization (grain-count) range measurements. See Appendix I for details.

### B. Scanning and Measurements

The plates were examined under  $53 \times 10$  magnification by an along-the-track scanning technique. Tracks were picked up 5 mm from the entrance edge. Because of the initial momentum spread, the  $K$ -meson tracks had a grain density ranging from 1.5 to 1.9 times minimum corresponding to an energy spread of about 42 Mev. The background tracks had a grain density ranging from 1.0 to 1.1 times minimum. The following types of measurements were carried out on the  $K$ -meson tracks:

1. All space angles with projected angles greater than  $2^\circ$  were measured up to a residual range of 3 mm (i.e.,  $T_K > 20 \text{ Mev}$ ).
2. For scattering events with visible-energy release, such as prongs or distinct change in ionization, grain counts with 3% to 5% statistics were carried out before and after the interaction. This measurement was also performed on *all* scattering events with space angle greater than  $40^\circ$  (large-angle elastic- and inelastic-scattering events).
3. All prongs from a  $K$ -meson interaction were identified and their ranges measured.
4. For those interactions in which none of the prongs were identified as a  $K$  meson, the mass of the primary particle was measured by multiple Coulomb scattering *vs* grain count (charge-exchange scattering events).
5. For events in which the secondary particle was near minimum ionization, grain counts on the primary and secondary were carried out which identified the event as a decay in flight. (In the case of a decay in flight of a  $\tau$  meson or  $K_{\mu 3}$  with low-energy  $\mu$  mesons, identifications were obvious.)

### C. Classification of Events

Throughout this work an attempt has been made to classify each event as elastic, inelastic, charge-exchange, or decay-in-flight.

Elastic interactions refer to those cases when the  $K$  meson interacted with the nucleus as a whole, and energy and momentum were conserved. In colliding

<sup>3</sup> Igo, Ravenhall, Tieman, Chupp, Goldhaber, Goldhaber, Lannutti, and Thaler, Phys. Rev. **109**, 2133 (1958), following paper.

with a light nucleus in emulsion this could mean a considerable energy loss but would result in a visible recoil. Using the range-energy data of Reynolds and Zucker<sup>4</sup> for nitrogen and the kinematics of the scattering, we could identify this type of event.

The measurement technique used to determine energy losses could reliably detect energy changes equal or greater than 10%.  $\Delta T/T \geq 10\%$  was thus chosen as a criterion for inelastic events. This classification is not rigorously correct because it is possible to excite low-lying rotational levels of the nuclei. Thus a  $K$  meson could have lost several Mev in such an inelastic-scattering process, and the loss would not have been detected. Consequently, the scattering would have been classified as elastic. Furthermore, in the high-energy interval the resolution is such that it is possible for the  $K$  meson to knock out or cause the evaporation of one or two nucleons and yet have an energy loss of less than 10%. Three such events were found which had an energy loss of less than 10% and yet emitted an evaporation-type proton. These were included among the *inelastic events*. To correct somewhat for the corresponding events giving neutron emission, these events were weighted by a factor of two in any distribution of events. This was actually a small correction among the 284 inelastic events found in all the systematic scanning. It is difficult to make a reliable estimate of the number of such events to be expected. However, since the Pauli exclusion principle inhibits low-energy-momentum transfers for scatterings off single nucleons, one would not expect a large fraction of scattering events with energy losses less than 10%. Thus we feel that our reaction-cross-section determination (excluding nuclear-level excitation) is not seriously affected by the 10% cutoff criterion.

In those cases classified as charge exchanges, considerable effort was expended to ascertain that the  $K$  meson was not among the visible prongs. If a prong was longer than 3 mm, its identity was established by direct measurement of scattering or ionization properties. If shorter, proof that it was not a  $K$  meson was based on the fact that no decay product was seen. This proof was quite good provided the track ended at least 20 microns from either surface of the emulsion. With the development used,  $K$ -meson decay secondaries had grain densities at least 21 grains per 100 microns. It was found that an experienced observer could find secondaries with nearly 100% efficiency if clear of either surface. At the surface the efficiency drops to about 80%. In this experiment only two doubtful events were found with prongs ending near the surface. These prongs had a range less than 1 mm. This is to be compared with all our other inelastic events in which only one case was found with a scattered  $K$ -meson range as low as 2 mm. All other scattered  $K$  mesons

had ranges greater than 4 mm. It thus appears safe to assume that these unknown prongs were not  $K$  mesons.

The classification of an event as a charge-exchange scattering rather than an absorption of a  $K$  meson, which would violate the  $\Delta S=0$  rule, was based on the visible-energy release which never exceeded the kinetic energy of the incoming  $K$  meson. Strong supporting evidence (see Sec. V-E) comes from the similarity between the stars produced by noncharge-exchange inelastically scattered mesons and the events classified as charge-exchange scattering events.

### III. CONSERVATION OF STRANGENESS

One effect of great interest in this work is the fact that so far no positive  $K$ -meson interaction has been observed in which the  $K$  meson gives up its rest energy. The limits can therefore be expressed as no case was observed in 304 inelastic interactions reported here. This characteristic behavior of the positive  $K$  meson supports the scheme presented by Gell-Mann and others<sup>5</sup> for a particle of positive strangeness. According to these schemes, it is not possible for a  $K^+$  meson to produce any of the known hyperons in a strong reaction because it would require a strangeness change of two, which violates the selection rule that  $\Delta S=0$  in strong reactions.

No evidence was found for the production of any hyperon-type particle (which would have to be of strangeness  $+1$ ) or for an excited fragment containing a bound  $K$  meson.<sup>6</sup> The metastability and decay of such fragments has been discussed by Pais and Serber.<sup>7</sup>

### IV. $K$ -HYDROGEN CROSS SECTION

Among the interactions of  $K^+$  mesons with emulsion nuclei, those with hydrogen are of special interest in studying  $K$ -nucleon forces. We identify these events by checking momentum and energy conservation, as well as coplanarity of the three prongs involved (i.e., the incoming  $K$  meson, the scattered  $K$ , and the recoil proton). In scanning along 283.7 m of  $K^+$  track in the energy region 20 to 220 Mev, we have found 13  $K$ -H interactions giving a mean free path of  $\lambda_{KH}=21.8$  m, which corresponds to a cross section of 14.4 mb. To improve the statistics we are including 30 events available from other published work with emulsion (Göttingen, 14 events; Padova, 6 events; Brookhaven, 4 events; Dublin, 2 events; Berkeley-Massachusetts Institute of Technology, 2 events; Rochester, 1 event; and Bristol, 1 event).<sup>8</sup> We evaluated the cross section

<sup>5</sup> M. Gell-Mann and A. Pais, *Proceedings of the Glasgow Conference on Nuclear and Meson Physics* (Pergamon Press, London, 1955); T. Nakano and K. Nishijima, *Progr. Theoret. Phys. (Japan)* **10**, 581 (1953); R. G. Sachs, *Phys. Rev.* **99**, 1573 (1955); M. Goldhaber, *Phys. Rev.* **92**, 1927 (1953); **101**, 433 (1956).

<sup>6</sup> Fry, Schneps, and Swami, *Phys. Rev.* **99**, 1951 (1955).

<sup>7</sup> A. Pais and R. Serber, *Phys. Rev.* **99**, 1551 (1955).

<sup>8</sup> Communications of the Bristol, Dublin, University of California, Göttingen, and Padova groups, Turin Conference, September, 1956 (unpublished); Biswas, Ceccarelli-Fabbrichesi, Ceccarelli, Cresti, Gottstein, Varshneya, and Waloschek, *Nuovo cimento* **1**, 137 (1957); B. Sechi-Zorn and G. T. Zorn (private communication).

<sup>4</sup> H. L. Reynolds and A. Zucker, *Phys. Rev.* **96**, 393 (1954).

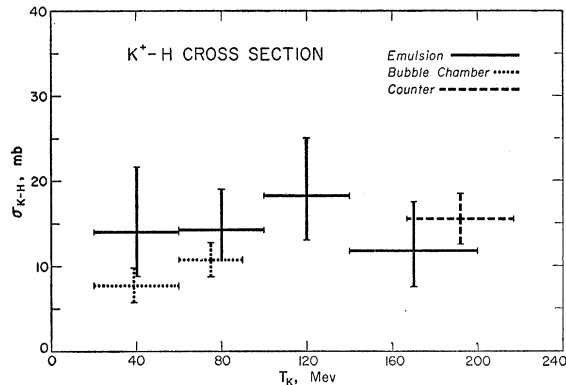


FIG. 2. The  $K^+$ -H cross section as a function of kinetic energy.

in four energy intervals. These results are shown in Fig. 2. The statistics are still poor, but these data are consistent with a constant cross section in the interval 20 to 200 Mev. The mean cross section over the total interval is  $14.5 \pm 2.2$  mb. Shown also on the plot for comparison are the results of Meyer *et al.*<sup>9</sup> (propane bubble chamber)— $9.4 \pm 1.7$  mb for the interval 20 to 90 Mev—and the counter result of Kerth *et al.*<sup>10</sup>— $15.4 \pm 3.0$  mb at  $192 \pm 25$  Mev. The propane bubble chamber result is somewhat lower than the emulsion result in the same energy region, but the difference is probably not statistically significant.

The angular distribution of all the data is shown in Fig. 3. In Figs. 3(a) and 3(b) the events have been plotted in two energy intervals below and above 100 Mev. In Fig. 3(b) the bubble-chamber data have been included. The angular distribution of the emulsion data is consistent with  $S$ -wave scattering in both energy intervals. In Fig. 3(c) we combine the data of both energy intervals. The new data weaken the earlier

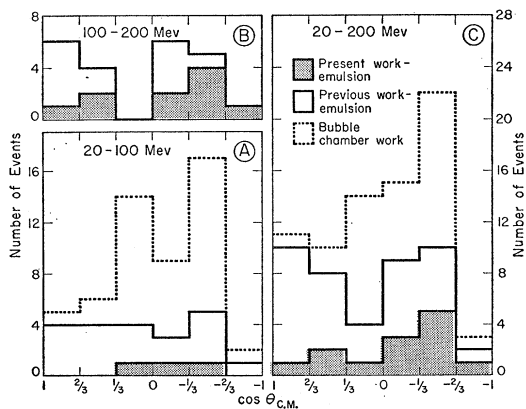


FIG. 3. Angular distribution of the  $K^+$ -H scattering in the center-of-mass system. Events from all sources have been added together. (a) Emulsion and bubble-chamber data, 20 to 100 Mev. (b) Emulsion data, 100 to 200 Mev. (c) Combined data, 20 to 200 Mev.

<sup>9</sup> Meyer, Perl, and Glaser, *Phys. Rev.* **107**, 279 (1957).

<sup>10</sup> Kerth, Kycia, and Van Rossum (private communication).

conclusion discussed in the literature<sup>8,11,12</sup> that the  $K$ - $p$  angular distribution indicated a rise in the forward direction compatible with a superposition of Coulomb scattering upon  $S$ -wave repulsive scattering. The lack of events in the first cosine interval of the bubble-chamber data is due to an experimental cutoff as discussed by Meyer *et al.*<sup>9</sup> The drop in the differential cross section in the cosine interval  $-\frac{2}{3}$  to  $-1$  is observed by both experiments and is not due to any experimental bias.

## V. INELASTIC INTERACTIONS

### A. Energy Dependence of Inelastic Interaction Cross Section

In Table I we have listed the inelastic-scattering events, i.e.,  $\Delta T/T \geq 10\%$ , charge-exchange-scattering events, elastic-scattering events with  $\theta_{\text{lab}} > 40^\circ$ , and  $K$ -H scattering events. The data have been divided into five energy intervals, and the corresponding path length scanned in each energy interval is listed. Source Be-MIT is data previously published.<sup>2</sup> Sources Be

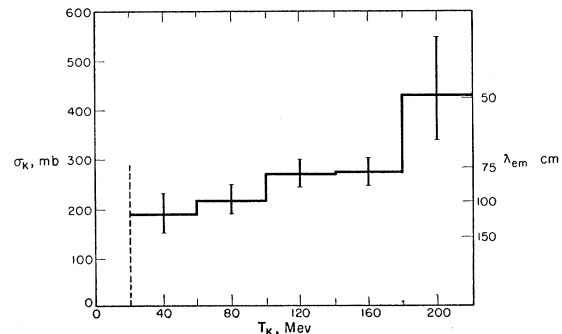


FIG. 4. Reaction cross section in emulsion as a function of incident kinetic energy.

and Bo are data obtained in the present work at Berkeley and Bologna, respectively, in systematic along-the-track scanning. Source Be(s) was data obtained in the present work at Berkeley in which additional  $K$ -meson tracks were followed in a search for charge-exchange scattering,  $K$ -hydrogen scattering events, and decays in flight, only. By not analyzing the elastic and inelastic scattering events, we were able to speed up the work considerably and increase the statistics on the type of events mentioned above.

The data of sources Be-MIT, Be, and Bo were used to obtain the variation of the reaction cross section for inelastic interactions with energy. These data are shown in Fig. 4, which indicates a rise of the reaction cross section with energy. The rise in the last energy interval, 180 to 220 Mev, is especially interesting because it is near the threshold for pion production

<sup>11</sup> Biswas, Ceccarelli-Fabbrichesi, Ceccarelli, Gottstein, Varshneya, and Waloschek, *Nuovo cimento* **5**, 123 (1957).

<sup>12</sup> Cocconi, Puppi, Quareni, and Stanghellini, *Nuovo cimento* **5**, 172 (1957).

TABLE I. Experimental data (20 to 220 Mev).

Energy interval (Mev)	Average energy (Mev)	Source	Path length (meters)	Inelastic		Number of events Charge-exchange		Elastic, $\theta > 40^\circ$	K-H
				Total	With no prongs <sup>a</sup>	Total	With no prongs		
20 to 60	44	Be-MIT	11.1	8	2	1	0	5	0
		Bo	10.8	10	9	1	1	8	0
		Be <sup>b</sup>	8.1	5	5	0	0	5	0
		Combined	30.0	23	16	2	1	18	0
60 to 100	81	Be(s)	4.5	...	...	0	0	...	0
		Be-MIT	16.3	10	3	3	0	10	0
		Bo	22.1	16	7	6	2	5	1
		Be <sup>b</sup>	13.4	18	9	0	0	5	2
100 to 140	120	Combined	51.8	44	19	9	2	20	3
		Be(s)	8.7	...	...	1(+1) <sup>c</sup>	0(+1)	...	1
		Be-MIT	8.8	2	1	0	0	0	2
		Bo	33.2	31(+1)	18(+1)	8	2	1(+1)	1
140 to 180	157	Be <sup>b</sup>	30.9	45	7	8	0	5	3
		Combined	72.9	78(+1)	26(+1)	16	2	6(+1)	7
		Be(s)	23.7	...	...	7	2	...	1
		Be-MIT	0.4	0	0	0	0	0	0
180 to 220	192	Bo	21.6	30	8	8	3	1	0
		Be <sup>b</sup>	49.1	43	6	12	2	0	2
		Combined	71.1	73	14	20	5	1	2
		Be(s)	40.0	...	...	7	0	...	1
Totals		Be-MIT	...	...	...	...	...	...	...
		Bo	1.2	3	0	0	0	0	0
		Be <sup>b</sup>	9.2	16	4	2	0	1	1
		Combined	10.4	19	4	2	0	1	1
Totals		Be(s)	7.4	...	...	1	0	...	0
		Be-MIT	36.6	20	6	4	0	15	2
		Bo	88.9	90(+1)	42(+1)	23	8	15(+1)	2
		Be <sup>b</sup>	110.7	127	31	22	2	16	8
Totals		Combined	236.2	237(+1)	79(+1)	49	10	46(+1)	12
		Be(s)	84.3	...	...	16(+1)	2(+1)	...	3

<sup>a</sup> With no prongs other than the K meson.  
<sup>b</sup> Elastic scatterings  $> 2^\circ$  were measured for part of the path length and are discussed in the following paper (reference 3) by Igo *et al.*  
<sup>c</sup> Numbers in parentheses are doubtful.

(225 Mev on free protons); Zorn *et al.*<sup>13</sup> confirm these results in the last energy interval with improved statistics.

**B. K-Nucleon Cross Section**

The inelastic interaction of high-energy neutrons with heavy nuclei can be described in terms of a simple model in which the nucleons within the nucleus are assumed to act as independent scattering centers, unaffected by their neighbors.<sup>14,15</sup> The nucleus is considered as a degenerate Fermi-Dirac gas of neutrons and protons without mutual interaction. This model is suited to describe the  $K^+$ -scattering process for the following reasons. The mean de Broglie wavelength for the K mesons in the energy interval under consideration is of the order of the nucleon size. The observed interaction cross section for  $K^+$  mesons is small (0.3 to 0.5 times geometric).

Applying this model, we can deduce the cross section for an elementary collision with a single nucleon from the inelastic scattering cross section with complex nuclei. According to this model an inelastic collision

occurs when the K meson, on traversing a complex nucleus, scatters elastically off one of its nucleons. The probability of such an event depends on the cross sections for  $K-p$  and  $K-n$  scattering,  $\sigma_{Kp}$  and  $\sigma_{Kn}$ , respectively. The average cross section per nucleon ( $\bar{\sigma}$ ) is then given by:

$$\bar{\sigma} = [Z\sigma_{Kp} + (A-Z)\sigma_{Kn}] / A. \tag{1}$$

To deduce a value of  $\bar{\sigma}$  from the mean free path for inelastic interaction in emulsion, a number of effects must be considered:

1. In the first approximation we can consider the emulsion as a collection of free nucleons. The resulting value for the K-nucleon cross section is given as  $\bar{\sigma}_1$  in Table II.

2. The shading effect. To take into account the shading of nucleons, we proceeded as follows: using  $\bar{\sigma}$  as a parameter, we have calculated a cross section for an inelastic interaction for each element in the emulsion according to the optical model.<sup>14,15</sup> These individual cross sections were combined to give the mean free path in nuclear emulsion,  $\lambda$ , according to the equation

$$\lambda = 1 / \sum_i (N_i \sigma_i), \tag{2}$$

where  $N_i$  is the number of nuclei per  $\text{cm}^3$  of the  $i$ th element and  $\sigma_i$  is the inelastic cross section for the  $i$ th

<sup>13</sup> B. Sechi-Zorn and G. T. Zorn (private communication) have observed 43 meters in the energy interval 190-210 Mev and find a mean free path of  $54 \pm 6$  cm.

<sup>14</sup> M. Goldberger, Phys. Rev. **74**, 1269 (1948).

<sup>15</sup> B. Rossi, *High-Energy Particles* (Prentice-Hall, Inc., Englewood Cliffs, New Jersey, 1952), p. 359.

TABLE II. Successive estimates of the  $K$ -nucleon cross section.

Energy interval (Mev)	Average energy (Mev)	Mean free path (cm)	$\sigma_{\text{emul}}$ (mb)	$\bar{\sigma}_1$ (mb)	$\bar{\sigma}_2$ (mb)	$\bar{\sigma}_3$ (mb)	$\bar{\sigma}_4$ (mb)	$\bar{\sigma}_5$ ( $V=25$ Mev) (mb)	C.E.	
									Non-C.E.	
20 to 60	44	$120_{-24}^{+30}$	$178_{-35}^{+42}$	$3.7_{-0.7}^{+0.9}$	$4.6_{-1.2}^{+1.6}$	$6.1_{-1.4}^{+2.2}$	$10.9_{-2.5}^{+3.9}$	... <sup>a</sup>	$0.08_{-0.05}^{+0.10}$	$0.21 \pm 0.08$
60 to 100	81	$98_{-12}^{+15}$	$217 \pm 30$	$4.5 \pm 0.6$	$6.0 \pm 1.1$	$6.9_{-1.2}^{+1.5}$	$9.1_{-1.6}^{+2.0}$	$10.6_{-1.8}^{+2.3}$	$0.22_{-0.05}^{+0.06}$	$0.24 \pm 0.05$
100 to 140	120	$77_{-7}^{+9}$	$277 \pm 28$	$5.7 \pm 0.6$	$8.4 \pm 1.1$	$9.4_{-1.5}^{+1.8}$	$11.3_{-1.8}^{+2.2}$	$11.9_{-1.9}^{+2.3}$	$0.24 \pm 0.05$	$0.09_{-0.05}^{+0.09}$
140 to 180	157	$77 \pm 8$	$277 \pm 29$	$5.7 \pm 0.6$	$8.4_{-1.1}^{+1.4}$	$9.2_{-1.3}^{+2.0}$	$10.5_{-1.5}^{+2.3}$	$10.8_{-1.5}^{+2.4}$		
180 to 220	192	$50_{-11}^{+13}$	$430_{-93}^{+116}$	$8.9_{-1.9}^{+2.4}$	$(18.5_{-7.2}^{+8.0})^b$	$(19.0_{-7.5}^{+8.5})^b$	$(21_{-8}^{+10})^b$	$(22_{-9}^{+10})^b$		

<sup>a</sup> In this energy interval the correction is extremely sensitive to the  $K$ -nucleon potential, making this value unreliable.

<sup>b</sup> These results must be treated with caution because the method used to obtain  $\sigma_2$  is unreliable for large cross sections.

element. The summation is taken over all elements of Ilford G-5 emulsion, excluding hydrogen. Hence one obtains  $\bar{\sigma}$  as a function of  $\lambda$  under the assumption that  $\bar{\sigma}$  is the same for each element. Thus, from the experimental values of the mean free path  $\lambda$ , we obtain  $\bar{\sigma}_2$  as given in Table II. The results given here are obtained by using  $R=r_0A^{1/3}$  with  $r_0=1.2 \times 10^{-13}$  cm.

The cross section for the highest energy interval must be considered as a crude approximation only, because the model used to calculate the effects of nucleon shading is applicable only when the interaction cross section is small.

3. The Coulomb repulsion effect. To allow for the decrease in the observed cross section ( $\sigma_{i \text{ obs}}$ ) from Coulomb repulsion, we used the approximation<sup>16</sup>

$$\sigma_{i \text{ obs}} = \sigma_i \left[ 1 - \frac{Z_i e^2}{(R_i + \lambda) T} \right], \quad (3)$$

where  $R_i$  is the nuclear radius of the  $i$ th element,  $Z_i$  is its charge,  $\lambda$  is the de Broglie wavelength of the incident  $K$  meson, and  $T$  is its kinetic energy. Substituting  $\sigma_{i \text{ obs}}$  for  $\sigma_i$  in Eq. (2), and calculating  $\bar{\sigma}$  as a function of  $\lambda$  for each energy interval, we obtain the values  $\bar{\sigma}_3$ , as given in Table II.

4. The Pauli-exclusion-principle effect. The Pauli exclusion principle limits the number of small-energy transfers to bound nucleons. Thus the cross section for interaction with a nucleon in a complex nucleus will be less than that with a free nucleon by a factor  $f(T)$ , depending on the  $K$ -meson energy,  $T$ . The factor  $f(T)$  has been calculated by Sternheimer<sup>17</sup> for various incident  $K$ -meson energies. Sternheimer has treated the nucleons within the nucleus as forming a degenerate Fermi-Dirac gas with a maximum Fermi energy of 25 Mev and has assumed the  $K$ -nucleon differential cross sections to be isotropic. Applying Sternheimer's results, we obtain  $\bar{\sigma}_4$  in Table II.

5. The repulsive nuclear potential. If the  $K$ -meson experiences a repulsive nuclear potential, the Pauli exclusion principle factor  $f(T)$  must be applied to

$T_{\text{in}}$ , the kinetic energy inside the nucleus, where  $T_{\text{in}} = T - V$ , and  $V$  is the combined Coulomb ( $V_C$ ) and nuclear ( $V_N$ ) repulsive potential. Taking  $V = +25$  Mev, for example, we obtain  $\bar{\sigma}_5$ , as given in Table II. The choice of magnitude of the repulsive nuclear potential has a large effect on the cross section,  $\bar{\sigma}_5$ , in the low-energy interval but this is not so critical for  $T_K > 100$  Mev. This is demonstrated in Fig. 5(a) where the cross section is plotted as a function of  $V$ . For  $V=0$  the value of  $\bar{\sigma}_5$  is identical with  $\bar{\sigma}_4$ . This model breaks down for the evaluation of the cross section for  $K$  mesons with kinetic energies close to the value of the potential itself. Thus the results obtained for the energy interval 20 to 60 Mev are not reliable.

The results for the energy interval 60 to 180 Mev have been combined and a mean value of  $\bar{\sigma}_5$  has been plotted in Fig. 5(b) as a function of  $V$ . In this energy interval we consider  $\bar{\sigma}_5$  to be the final best value of  $\bar{\sigma}$  the average  $K$ -nucleon cross section. Using the average value of  $\sigma_{Kp}$  given in Sec. IV and Eq. (1), we have calculated the  $K$ -neutron cross section, which is also plotted in Fig. 5(b).

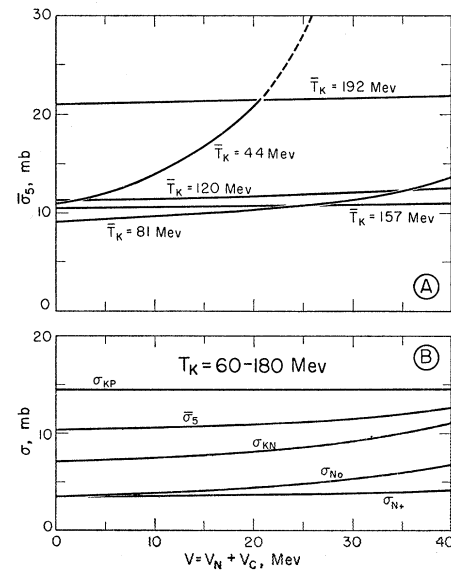


FIG. 5. Elementary cross sections as a function of the combined nuclear and Coulomb potential. (a) The effect of the potentials on the average  $K$ -nucleon cross section for various incident energies. (b) The effect of the potentials on the elementary scattering cross sections in the energy interval 60 to 180 Mev.

<sup>16</sup> J. M. Blatt and V. F. Weisskopf, *Theoretical Nuclear Physics* (John Wiley and Sons, Inc., New York, 1952), p. 350.

<sup>17</sup> R. M. Sternheimer, *Phys. Rev.* **106**, 1027 (1957). See also I. G. Ivanter and L. B. Okun, *J. Exptl. Theoret. Phys. (U.S.S.R.)* **32**, 402 (1957); English translation: *Soviet Physics JETP* **5**, 340 (1957).

The ratio of charge-exchange events to noncharge-exchange inelastic events is practically constant in this energy interval and is equal to  $0.227 \pm 0.029$ . This ratio was used to obtain the cross section for charge-exchange scattering,  $\sigma_n^0$ , which is also shown in Fig. 5(b). Since  $\sigma_{Kn} = \sigma_n^0 + \sigma_n^+$ , where  $\sigma_n^+$  is the cross section for direct scattering off neutrons,  $\sigma_n^+$  was deduced and is presented in the same figure.

### C. Angular Distribution of $K^+$ Inelastic Scattering Events

As discussed in Sec. V-B, the inelastic scattering has been assumed to be scattering off single nucleons in complex nuclei. It can thus be expected that the differential cross section for inelastic scattering can be related to the differential cross section for  $K$ - $p$  and  $K$ - $n$  scattering. Figures 6(a) and (b) give the angular distribution of  $K$  scattering events in the laboratory

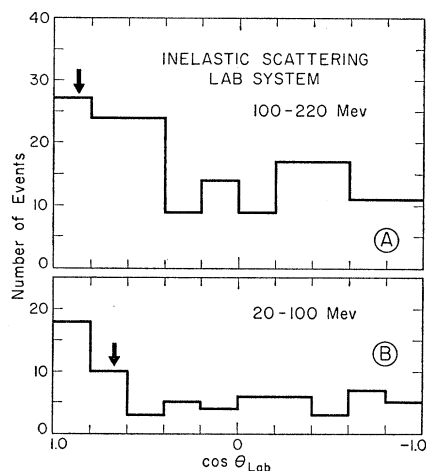


FIG. 6. Inelastic-scattering events in laboratory system, (a) for energy interval 100 to 220 Mev; (b) for energy interval 20 to 100 Mev.

system for incident  $K$ -meson energies above and below 100 Mev, respectively. From these data we can obtain the angular distribution in the center-of-mass system to the first approximation if we (a) neglect refraction effects on the  $K$ -meson angles from the  $K$ -nucleus potential, and (b) assume the  $K$ -nucleon collisions to occur with a nucleon at rest.<sup>18</sup> Figures 7(a) and (b) give the resulting angular distribution in the center-of-mass system. In the backward hemisphere the distribution should now approximate the  $K$ -nucleon differential cross section. In the forward hemisphere the Pauli exclusion principle tends to suppress the cross section strongly, an effect which is enhanced by a repulsive potential. The arrows on Figs. 6 and 7 indicate the effective average cutoff angle<sup>17</sup> below which scatters

<sup>18</sup> Comparison with Monte Carlo calculations for similar processes have shown this to be a good approximation (private communication by G. Puppi).

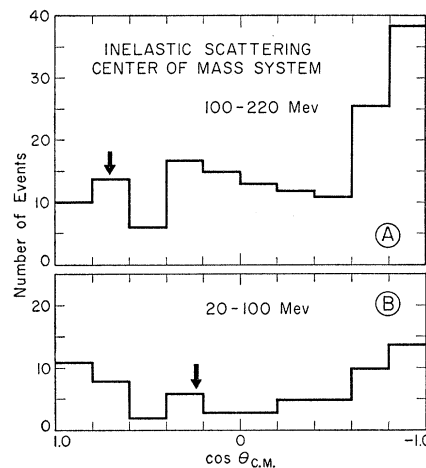


FIG. 7. Inelastic-scattering events in center-of-mass system, (a) for energy interval 100 to 220 Mev; (b) for energy interval 20 to 100 Mev.

are prohibited by the Pauli exclusion principle. Experimentally we observe, however, a number of events at small scattering angles, where the Pauli exclusion principle should be most effective. These events can be partly explained as corresponding to  $K$  mesons that have undergone two successive collisions.<sup>19</sup> In some of these events the  $K$  meson suffered large energy losses as shown in Fig. 8 lying above curve C. This may be

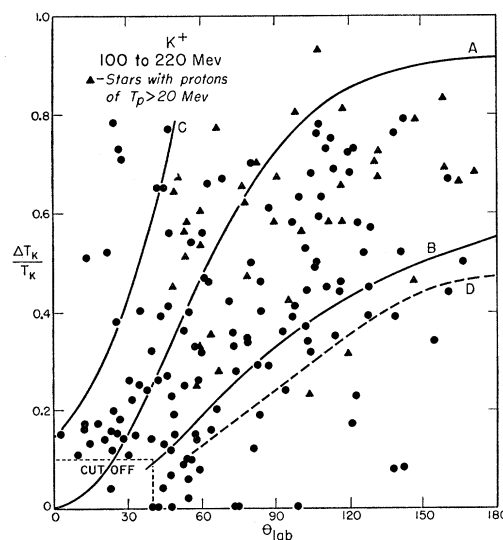


FIG. 8. Fractional energy loss vs laboratory scattering-angle correlation-diagram for scatters in complex nuclei. Curve A is for free protons at rest. Curves B and C show limiting cases of scattering from nucleons moving with momentum 218 Mev/ $c$  opposite to and in the direction of free motion of the  $K$  meson, respectively. Curve D is for a free  $\alpha$  particle at rest. The dashed cutoff lines correspond to the 10% resolution cutoff and 40° angular cutoff. The triangles indicate events with "knock-on" protons ( $T_p > 20$  Mev).

<sup>19</sup> The number of  $K$  particles undergoing two collisions is estimated to be approximately 25% [Brueckner, Serber, and Watson, Phys. Rev. 84, 258 (1951)].

taken as evidence that these  $K$  mesons made more than one collision before leaving the complex nucleus.

The backward peaking for the high-energy interval, indicating  $P$ -wave scattering, has also been observed by other groups using more elaborate transformations to the center-of-mass system.<sup>11,20,21</sup>

#### D. Energy Loss in Inelastic Collisions

The characteristic feature of the positive  $K$ -meson inelastic scattering is that the energy loss is in general smaller than expected for collisions with a free nucleon. The energy loss does, however, increase with increasing scattering angle as expected in collisions with single nucleons. This behavior can be contrasted with the inelastic scattering of pions, which always suffer large energy losses. The large energy loss in pion scattering can be explained on the basis of the very large scattering cross section near the  $\frac{3}{2}$ ,  $\frac{3}{2}$  pion-nucleon resonance. The pions undergo several collisions inside the complex nucleus and finally emerge with a low energy for which the scattering cross section is small. For the  $K$ -meson case under consideration here, the  $K$ -nucleon scattering cross section is small so that in the majority of the interactions only a single collision will occur. The small energy loss observed in  $K$ -meson scattering can be understood in terms of a repulsive  $K^+$  nuclear potential, as has been pointed out already.<sup>11,20</sup>

Figure 8 shows the correlation between the fractional energy loss  $\Delta T_K/T_K$  and the scattering angle  $\theta_{lab}$  of the  $K$ -meson scattering events we have found in the energy interval 100 to 220 Mev. Curve  $A$  shows the energy loss in  $K$ - $p$  collisions with free protons as a function of the scattering angle  $\theta_{lab}$ . Curves  $B$  and  $C$  show the two limiting cases of collisions with a nucleon in motion having a maximum Fermi momentum of 218 Mev/ $c$ . The two curves  $B$  and  $C$  correspond to a nucleon moving opposite to and in the direction of motion of the  $K$  meson, respectively. As can be clearly seen from Fig. 8, the majority of the events are inside the limits imposed by curves  $B$  and  $C$ . The average-fractional-energy loss versus scattering-angle curves lies, however, below curve  $A$  in accordance with a repulsive  $K$ -nucleus potential. It has been suggested that the reduced energy loss of  $K^+$  mesons may be due to collisions with heavier nuclear clusters such as  $\alpha$  particles.<sup>11</sup> Curve  $D$  shows the fractional energy loss for collisions with free  $\alpha$  particles. It can be seen that the scattering events do not follow this curve. There is thus no evidence from the present work that the smaller energy losses are due to  $K$ - $\alpha$  interactions. It should also be noted that carbon or oxygen disintegrations by  $K$  mesons<sup>22,23</sup> need not imply specific  $K$ - $\alpha$

<sup>20</sup> Baldo-Ceolin, Cresti, Dallaporta, Grilli, Guerriero, Merlin, Salandin, and Zago, Nuovo cimento **5**, 402 (1957).

<sup>21</sup> Bhowmik, Evans, Nilsson, Prowse, Anderson, Keefe, Kerman, and Losty, Nuovo cimento **6**, 440 (1957).

<sup>22</sup> Anderson, Keefe, Kerman, and Losty, Nuovo cimento **4**, 1198 (1956).

<sup>23</sup> Hoang, Kaplan, and Cester, Phys. Rev. **107**, 1698 (1957).

collisions. Such disintegrations are also observed with  $\gamma$  rays,<sup>24</sup>  $\pi$  mesons,<sup>25</sup> protons,<sup>26</sup> and neutrons.<sup>27</sup> The events indicated by a triangle  $\Delta$  in Fig. 8 are those inelastically scattered  $K^+$  mesons with an associated fast "knock-on" proton ( $T_p > 20$  Mev). Most of these events correspond to quasi-elastic scattering events, i.e., the angular and energy correlations of both the  $K$  meson and the proton agree roughly with the kinematics of  $K$ -nucleon scattering. The fact that the quasi-elastic events are distributed uniformly among all inelastic events further strengthens the hypothesis that the mechanism for inelastic  $K$ -meson scattering proceeds through elastic collision with a single nucleon.

In Fig. 9 the mean fractional energy loss  $\Delta T_K/T_K$  is given as a function of the incident  $K$ -meson energy. The  $\Delta T_K/T_K$  values vary from 0.2 at about 40 Mev to 0.5 at about 200 Mev. The curves correspond to an estimate of  $\Delta T_K/T_K$  as modified by various values of a  $K$ -nucleus repulsive potential. In this estimate an isotropic angular distribution for the  $K$ -meson scattering was assumed, and the effect of the Pauli exclusion principle was applied. Here again a repulsive potential is indicated, with a best estimate of  $V_C + V_N \sim 30$  Mev.

#### E. Comparison of Charge-Exchange and Noncharge-Exchange Events

The classification of events in which the charged  $K$  meson is not re-emitted as "charge-exchange scattering" is based on the assignment of isotopic spin  $T = \frac{1}{2}$  to the positive  $K$  mesons and the selection rule  $\Delta S = 0$  for strong interactions.<sup>5</sup> From the experimental point of view the evidence is as follows:

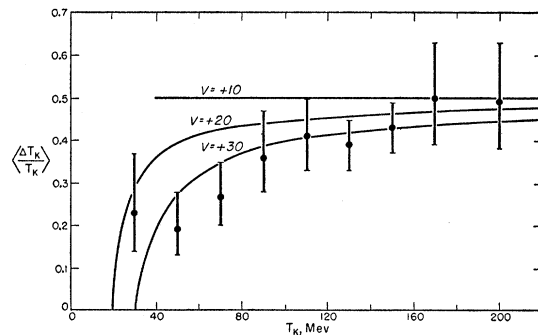


FIG. 9. Fractional energy loss versus kinetic energy of  $K$  meson for all inelastic events. Curves are expected behavior for various potentials  $V = V_n + V_c$ .

<sup>24</sup> Hanni, Telegdi, and Zunti, Helv. Phys. Acta **21**, 203 (1948); V. L. Telegdi and M. Eder, Helv. Phys. Acta **25**, 55 (1952); F. K. Goward and J. J. Wilkins, Proc. Phys. Soc. (London) **A64**, 201 and 1056 (1951); C. H. Millar and A. G. W. Cameron, Can. J. Phys. **31**, 723 (1953); S. D. Softky, Phys. Rev. **98**, 173 (1955).

<sup>25</sup> Bernardini, Booth, and Lederman, Phys. Rev. **83**, 1277 (1951); Della Corte, Fazzini, and Sona, Nuovo cimento **2**, 1345 (1955).

<sup>26</sup> J. L. Need, Phys. Rev. **99**, 1356 (1955).

<sup>27</sup> H. Aoki, Proc. Phys.-Math. Soc. Japan **20**, 755 (1938); L. L. Green and W. M. Gibson, Proc. Phys. Soc. (London) **A62**, 296 (1949).



1. In none of the interactions does the visible energy release exceed the kinetic energy of the  $K$  meson.

2. As shown below, the stars associated with the events in which a  $K$  meson is *not* re-emitted, resemble very closely the group of stars associated with noncharge-exchange inelastic scattering. Figures 10(a) and (b) show the energy distribution of prongs (considered as protons) from charge-exchange and noncharge-exchange events, respectively. Only events occurring at  $T_K \geq 100$  Mev have been included. Here prongs with range  $< 10\mu$  ( $T_p < 0.8$  Mev) have been omitted. Both distributions are consistent with an evaporation spectrum superimposed on a tail of energetic "knock-on" protons. Both curves correspond to nuclear temperature  $\tau = 2.6$  Mev, which was determined from the average energy loss in the noncharge-exchange inelastic scattering events  $\langle \Delta T_K \rangle = 64$  Mev. The prongs with kinetic energy less than 4 Mev [shaded regions in Fig. 10(a) and (b)] are presumably partly due to unidentified  $\alpha$  particles and partly to protons from light elements for which the evaporation theory is not applicable. The fact that the evaporation spectra from both charge-exchange and noncharge-exchange scattering events can be fitted by the same nuclear temperature indicates that the average energy loss is very similar in the two processes. Table III gives comparative data between the two types of processes. *A priori*, certain differences are expected between the two processes. In the charge-exchange process the nuclear excitation is initiated by a proton from the reaction (a)  $K^+ + n \rightarrow K^0 + p$ , while in the noncharge-exchange inelastic scattering the nuclear excitation can be initiated by either a proton or a neutron from the reactions (b)  $K^+ + p \rightarrow K^+ + p$ , and (c)  $K^+ + n \rightarrow K^+ + n$ . This difference gives rise to two effects:

(i) A charge excess among the nuclear evaporation particles from reaction (a) as compared with reactions (b) and (c) combined, due to the increased probability for proton emission.

(ii) A larger probability for fast-proton emission ("knock-on" protons) from the charge-exchange scattering reaction (a).

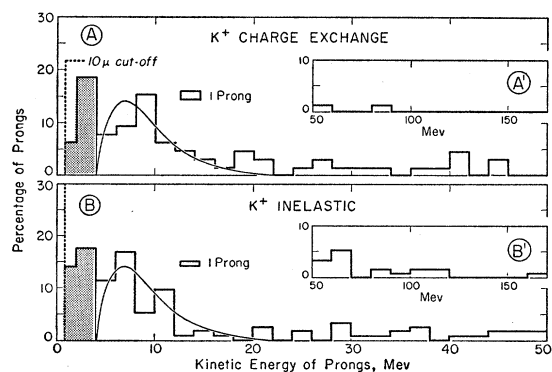


FIG. 10. Comparison of prong energies of charge-exchange stars with those of noncharge-exchange stars. Curves are evaporation spectra for excitation energy of 64 Mev.

TABLE III. Comparison of charge-exchange scattering events with noncharge-exchange inelastic scattering events, for  $T_K = 100$  to 220 Mev.

	Noncharge-exchange	Charge-exchange
No. of knock-on prongs/ total number of stars	$0.27 \pm 0.02$	$0.47 \pm 0.08$
No. of evaporation prongs/total number of stars	$0.51 \pm 0.04$	$0.71 \pm 0.12$
Visible knock-on energy <sup>a</sup> / total number of stars	$15.6 \pm 1.2$ Mev	$21.4 \pm 3.5$ Mev
Visible evaporation energy <sup>a</sup> /total number of stars	$7.0 \pm 0.5$ Mev	$9.8 \pm 1.6$ Mev
Visible knock-on energy <sup>a</sup> /No. of stars with knock-on prongs	$60.0 \pm 9.0$ Mev	$48 \pm 14$
Average energy loss	$64.2 \pm 4.9$	...

<sup>a</sup> These quantities include the binding energy.

Both of these effects have been observed and are given in Table III. It is interesting to note that the number of "knock-on" protons from reaction (a) is about twice that from reaction (b) and (c). The difference in the number of "knock-on" protons could be used to compute the  $K$ -neutron cross section. The present statistics do not warrant such a computation, but are certainly consistent with the  $K$ -neutron cross section ( $\sigma_{Kn}$ ) given in Sec. V-B.

## VI. DISCUSSION OF RESULTS

From the results of  $K^+$  scattering discussed in this paper, we draw the following conclusions:

(a) The cross section of the  $K$ -hydrogen elastic scattering appears to be energy-independent in the energy region 20 to 200 Mev. The differential  $K$ -H cross section as determined by  $K^+$  scattering off hydrogen in emulsions shows mainly  $S$ -wave scattering.

To analyze the combination of the emulsion data and bubble chamber data for  $K$ -hydrogen scattering, as shown in Fig. 3, one has to compensate for the fact that the identification of  $K$ -H scattering events in a propane bubble chamber becomes exceedingly difficult in the cosine interval 1 to  $\frac{2}{3}$ .

The decrease in the differential cross section in the interval  $-\frac{2}{3}$  to  $-1$  is not subject to experimental bias by either method. To fit such a distribution by partial wave expansion, one would have to include high angular momenta. It is, however, difficult to reconcile the energy-independent cross section with angular momenta terms higher than  $P$  wave. These arguments indicate that the  $K$ -H scattering in the energy interval under discussion is due mainly to  $S$ -wave scattering with possibly a small  $P$ -wave contribution. This, however, does not fully explain the large drop in the last angular interval observed in the differential cross section, which we would like to attribute in part to a statistical fluctuation.

The average  $K$ -nucleon cross section between 60 to 180 Mev is essentially energy-independent. The

TABLE IV. Reaction probabilities for  $K^+$ -nucleon scattering.

Reaction	Probabilities <sup>a</sup>
$K^+ + p \rightarrow K^+ + p$	$ A_1 ^2$
$K^+ + n \rightarrow K^+ + n$	$\frac{1}{4} A_1 + A_0 ^2$
$K^+ + n \rightarrow K^0 + p$	$\frac{3}{4} A_1 - A_0 ^2$

<sup>a</sup>  $A_1$  and  $A_0$  represent the  $T=1$  and  $T=0$  scattering amplitudes, respectively.

backward peaking observed in the differential cross section in the energy interval 100 to 220 Mev is most likely due to  $P$ -wave scattering. These two observations are not inconsistent because the angular distribution is more sensitive to a small  $P$ -wave component than is the energy dependence of the cross section.

We conclude, therefore, that the results in both the  $K$ -hydrogen scattering and the average  $K$ -nucleon scattering can be interpreted as predominantly  $S$ -wave scattering with a small  $P$ -wave contribution.

These results lead us to believe that the  $K$ -nucleon scattering is a short-range interaction and does not proceed through single  $\pi$ -meson exchange. The latter would require high angular-momenta contribution to the  $K^+$  scattering even at an energy below 100 Mev and would presumably result in a strongly energy-dependent cross section.

(b) The rise in the  $K$ -nucleon cross section observed in this work as well as that of Zorn *et al.*<sup>13</sup> in the energy interval 180 to 220 Mev can be interpreted as follows: (1)  $P$ -wave scattering becomes more significant at this higher energy. (2) This energy interval is near the pion-production threshold, and a rise in the cross section could be expected.

(c) A repulsive potential was necessary to explain the behavior of the fractional energy loss as a function of energy (Fig. 9). The magnitude of the nuclear potential was determined independently from an exact phase-shift analysis of the elastic-scattering data<sup>3</sup> to be of the order of 27 Mev. This result is in good agreement with the results shown in Fig. 9.

(d) Because the  $K$  meson is an isotopic spin doublet, the  $K$ -nucleon interaction can occur in both singlet and triplet isotopic spin states. Table IV gives the reaction probabilities for  $K^+$ -nucleon scattering.

It is of interest in this connection to examine the ratio of cross section for charge exchange to noncharge exchange inelastic scattering. As is shown in Table II, this ratio appears to remain constant with energy and equal to  $\sim \frac{1}{5}$  in the energy region  $T_K=60$  to 180 Mev. The ratio is based on 64 charge-exchange events obtained by following 268 meters of  $K$ -meson track. In the energy interval 20 to 60 Mev this ratio becomes  $\sim \frac{1}{10}$  on the basis of very poor statistics, namely, two charge exchange events in 34.5 meters of  $K^+$  meson track followed. A very similar result was obtained in the work of Hoang *et al.*<sup>23</sup> in an energy region  $T_K=30-65$  Mev

in which 0 to 2 change events were reported in  $\sim 45$  meters of  $K^+$  track followed.

From the present data we like to take the simplest approach to the  $K^+$ -nucleon scattering process and attribute it mainly to  $S$ -wave scattering. We thus assume the ratio of charge-exchange to noncharge-exchange scattering to be energy-independent and attribute the low value in the energy interval 20-60 Mev to a statistical fluctuation. As will be shown below, this leads to scattering principally in the  $T=1$  state. This approach is contrary to the point of view taken by Hoang *et al.* who, on the basis of the apparent small value of the charge-exchange scattering in the 30-65-Mev energy region, suggested a large contribution to the scattering in the  $T=0$  state.

We find that the ratio  $\sigma_{Kp}:\sigma_{Kn^+}:\sigma_{Kn^0}$  is equal to 3.6:1.5:1, if we assume a repulsive nuclear potential of 25 Mev and a Coulomb potential of 10 Mev. As can be seen in Fig. 5, this ratio is a function of the nuclear potential, but is consistent with an assumption that the scattering in the  $T=0$  state is small.

The calculated value of the average  $K$ -nucleon cross section for the energy interval 60 to 180 Mev with a nuclear potential of 25 Mev is  $11.8 \pm 1.3$  mb. In making this calculation, the existence of double scattering in the nucleus and refraction and reflection from the nuclear potential<sup>3</sup> have not been considered. Corrections due to these effects will tend to increase the cross section.

Expressing the above arguments quantitatively, we are now in a position to evaluate the  $S$ -wave phase shifts. Let us denote the  $K$ -nucleon phase shifts by  $\delta_0$  and  $\delta_1$  for  $S$  waves and isotopic spin  $T=0$  and  $T=1$  respectively, and by  $\delta_{01}$ ,  $\delta_{02}$ ,  $\delta_{11}$ ,  $\delta_{13}$  for  $p$  waves, where the first index is the isotopic spin  $T$  and the second index is twice the total angular momentum ( $2J$ ). The forward scattering amplitude in the isotopic spin state  $T$ , keeping only  $S$  and  $P$  waves, is then given by

$$f_T(0) = \frac{1}{k} (e^{i\delta_T} \sin\delta_T + 2e^{i\delta_{T3}} \sin\delta_{T3} + e^{i\delta_{T1}} \sin\delta_{T1}), \quad (4)$$

which yields

$$\text{Im}f_T(0) = \frac{1}{k} (\sin^2\delta_T + 2 \sin^2\delta_{T3} + \sin^2\delta_{T1}), \quad (5)$$

and

$$\text{Re}f_T(0) = \frac{1}{2k} (\sin 2\delta_T + 2 \sin 2\delta_{T3} + \sin 2\delta_{T1}). \quad (6)$$

We can now apply the further approximation that the  $P$ -wave phase shifts are small (based on the experimentally observed lack of energy dependence of the  $K$ -nucleon cross section). Thus terms involving the square or product of  $P$ -wave phase shifts can be neglected.

We obtain thus:

$$\sigma_{Kp} = \frac{4\pi}{k^2} \sin^2 \delta_1, \quad (7)$$

$$\sigma_{Kn^+} = \frac{4\pi}{k^2} \left| \frac{1}{2} (e^{i\delta_1} \sin \delta_1 + e^{i\delta_0} \sin \delta_0) \right|^2, \quad (8)$$

$$\sigma_{Kn^0} = \frac{4\pi}{k^2} \left| \frac{1}{2} (e^{i\delta_1} \sin \delta_1 - e^{i\delta_0} \sin \delta_0) \right|^2. \quad (9)$$

We shall now use the values  $\sigma_{Kp} = 14.5 \pm 2.2$  mb,  $\sigma_{Kn^+} = 5.8 \pm 3.1$  mb, and  $\sigma_{Kn^0} = 4.0 \pm 0.8$  mb which are obtained for  $V = V_N + V_C = 35$  Mev (see Fig. 5) and are valid in the energy region  $T_K = 60$ – $180$  Mev, as discussed above. We can use these cross sections to evaluate the  $S$ -wave scattering lengths  $a_T$  where  $a_T = \sin \delta_T / k$  assuming this quantity to be energy-independent.

Equation (7) becomes

$$\sigma_{Kp} = 4\pi a_1^2, \quad (7')$$

giving  $a_1 = -0.24 \pm 0.02$  in units of  $\hbar/m_\pi c$ . The negative sign is used in correspondence with a repulsive potential. We now make the further simplification that  $\delta_1$  and  $\delta_0$  are sufficiently small so that the phases in Eqs. (8) and (9) can be neglected.<sup>28</sup> Of these two cross sections,  $\sigma_{Kn^0}$  is known with greater precision and we thus solve for  $a_0$  from

$$\sigma_{Kn^0} = \pi (a_1 - a_0)^2. \quad (9')$$

This gives the two possible values  $a_0 = +0.014 \pm 0.03$  and  $a_0 = -0.49 \pm 0.03$ . The latter can be ruled out immediately by comparing with  $\sigma_{Kn^+}$ . Although  $\sigma_{Kn^+}$  is not determined to great precision, the alternative values of  $\sigma_{Kn^+}$  are 3.2 mb and 24.7 mb, respectively. These are obtained by solving for  $\sigma_{Kn^+}$  from

$$\sigma_{Kn^+} = \pi (a_1 + a_0)^2, \quad (8')$$

and by substituting  $a_1$  and the two possible values of  $a_0$ . This indicates clearly that the proper choice for  $a_0$  is  $a_0 = +0.014 \pm 0.03$ . To obtain information on the  $P$ -wave phase shifts, an analysis of the differential  $K$ -hydrogen cross section  $d\sigma_{Kp}/d\Omega$  would be required which we feel is premature on the basis of the presently available  $K$ -hydrogen scattering data (Fig. 3). Some corroboration of the assumption that the  $P$ -wave phase shifts are small can, however, be obtained from a quite different approach.

We can compute the real part of the optical potential from the expression<sup>29</sup>

$$V_N = -2\pi\rho_0 \left( \frac{1}{m_K} + \frac{1}{m_p} \right) \text{Re} \bar{f}(0), \quad (10)$$

<sup>28</sup> For instance, at  $T_K = 140$  Mev  $= m_\pi c^2$ ,  $\delta_1 = -26^\circ$  and the approximation  $\sin \delta_1 \approx \delta_1$  is still reasonable.

<sup>29</sup> See, for instance, Frank, Gammel, and Watson, Phys. Rev. **101**, 891 (1956).

where  $\rho_0$  is the nucleon density in the central region of the nucleus,<sup>30</sup>  $m_K$  and  $m_p$  are the  $K$ -meson, and nucleon masses, respectively, and  $\bar{f}(0)$  is the forward scattering amplitude as averaged over neutrons and protons in emulsion nuclei:

$$\begin{aligned} \bar{f}(0) &= \frac{1}{2.2} [f_p(0) + 1.2f_n(0)] \\ &= 0.73f_1(0) + 0.27f_0(0); \quad (11) \end{aligned}$$

we have used  $f_p(0) = f_1(0)$  and  $f_n(0) = \frac{1}{2}[f_1(0) + f_0(0)]$ . The units used for energy and length are  $m_\pi c^2$  and  $\hbar/m_\pi c$ , and we have taken  $\hbar = c = 1$ . If we again apply the small-phase-shift approximation and write  $b_T^+ = (1/k)(2 \sin \delta_{T3} + \sin \delta_{T1})$  for the nonspin-flip  $P$ -wave scattering length, we obtain

$$\begin{aligned} \text{Re} \bar{f}(0) &= 0.73[a_1 + b_1^+] + 0.27[a_0 + b_0^+] \\ &= -0.17 \pm 0.014 + 0.73b_1^+ + 0.27b_0^+, \quad (12) \end{aligned}$$

giving  $V_N$  (expressed in Mev) as  $V_N = 29.2 \pm 2.4 - 171(0.73b_1^+ + 0.27b_0^+)$  Mev, where the term in parentheses corresponds to the  $P$ -wave contributions. In comparing this value of  $V_N$  with the magnitude obtained by fitting the small-angle scattering data, in the following paper,<sup>3</sup>  $V_N = 27$  Mev, we see that the agreement with the contribution due to  $S$  waves alone ( $V_N = 29.2 \pm 2.4$ ) is very good. We could also proceed and obtain  $W$ , the imaginary part of the optical potential, which is related to  $\text{Im} \bar{f}(0)$  by an equation identical to Eq. (10) except that one must include the factor  $\eta$  due to the Pauli exclusion principle.<sup>17</sup> This step is taken in the following paper<sup>3</sup> where one goes in the reverse direction, namely, from  $W$  to  $\bar{\sigma}$ , where

$$\bar{\sigma} = (4\pi/k) \text{Im} \bar{f}(0).$$

#### ACKNOWLEDGMENTS

We wish to thank Dr. D. H. Stork and Mr. O. Price for their assistance in the design and setting up of the beam. The excellent support and cooperation given by Dr. E. Lofgren and the Bevatron crew was greatly appreciated. We are indebted to Dr. G. Puppi for a number of valuable discussions and to Dr. Geoffrey Chew for many helpful comments in connection with the phase-shift analysis. We are especially grateful to Mrs. Frances Glenn, Miss Graydon Hindley, Mr. D. H. Kouns, Miss Helen Probst, Miss Harriet Rice, Mrs. Catherine Toche, and the group at the University of Bologna for their constant assistance throughout this work.

#### APPENDIX I. IDENTIFICATION OF CHARGE EXCHANGE-EVENTS AND THE PROTON CONTAMINATION

For all interactions in which a  $K$  meson was not emitted as an interaction product, a mass measurement was performed on the primary track. The mass determination consisted of a grain-density and multiple-

<sup>30</sup> See Eq. (8) in the following paper (reference 3).

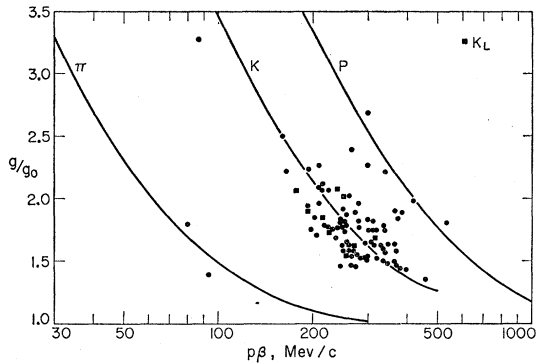


Fig. 11. Grain density *versus*  $p\beta$  for multiple-scattering measurements most of which were on primaries of charge exchanges.

Coulomb-scattering measurement. For tracks long enough to enable us to determine the variation of ionization *versus* residual range, an independent mass determination was performed by grain count. As an example we show in Fig. 11 a plot of  $p\beta$  obtained from the mean multiple-scattering angle *versus* the grain density for all measurements performed on the Berkeley data.

As discussed in Sec. II-B, we selected only those tracks to be followed whose grain density fell into the interval 1.5 to 1.9 times minimum ionization. Among the tracks followed we found a proton contamination of 1.8%. For the path length of protons observed and using a geometric mean free path of 36 cm ( $r_0=1.2 \times 10^{-13}$  cm), one expects ten inelastic proton events for the plates scanned in Berkeley. This is in good agreement with the results of the  $p\beta$  and grain-density measurements discussed above in which nine of the inelastic events were identified to be due to protons.

#### APPENDIX II. THE MEAN LIFE DETERMINATION

Since in the present experiment we have a source of  $K^+$  mesons that is very different from previous emulsion

experiments,<sup>31</sup> i.e.,  $T_K=390$  Mev at production,  $1.9 \times 10^{-8}$  sec proper time of flight to stack, and traversal of 87 g/cm<sup>2</sup> of Be, we have compiled the  $K^+$  decay events to obtain a  $K^+$  lifetime under these conditions. We have found 84 decays in flight; using the observed proper time of flight for all  $K$  mesons, we obtain a mean lifetime of

$$T = (1.59 \pm 0.16^{0.20}) \times 10^{-8} \text{ sec.}$$

This value is two standard deviations from the counter value  $(1.22 \pm 0.01) \times 10^{-8}$  sec.<sup>32</sup> It should be noted that in principle some of the disappearances in flight (i.e., charge exchanges with no visible prongs) could have been decays in flight in which the decay secondary was missed. However, almost all the disappearances occurred in the middle of the emulsion where there is little difficulty in locating decay products in the present stack. In addition, the fraction of the charge exchanges that are disappearances is consistent with what is expected from the fraction of noncharge-exchange inelastic scattering events that have no prongs other than the  $K$  meson. However, if one does consider all the disappearances in flight to be decays in flight (a situation which we certainly do not believe) the lifetime becomes  $(1.38 \pm 0.13^{0.15}) \times 10^{-8}$  sec. In addition, this would change the ratio of charge exchange to noncharge exchange in the interval 60 to 180 Mev from  $0.227 \pm 0.029$  to  $0.183 \pm 0.026$ .

In view of the new proposals that assert that the  $\tau-\theta$  puzzle may be accounted for by parity nonconservation, the most likely explanation for the difference between our observed lifetime and the counter result is that it is due to a statistical fluctuation.

<sup>31</sup> Iloff, Chupp, Goldhaber, Goldhaber, Lannutti, Pevsner, and Ritson, Phys. Rev. **99**, 1617 (1955); Bhowmik, Evans, Nilsson, Prowse, Anderson, Keefe, Kannan, Biswas, Ceccarelli, Waloschek, Hooper, Grilli, and Guerriero, Nuovo cimento **5**, 994 (1957); Davis, Hoang, and Kaplon, Phys. Rev. **106**, 1049 (1957).

<sup>32</sup> V. Fitch and R. Motley, Phys. Rev. **101**, 496 (1956); Alvarez, Crawford, Good, and Stevenson, Phys. Rev. **101**, 503 (1956).